Inorg. Chem. **2007**, *46*, 1645–1654

Characterization of Co–C Bonding in Dichlorovinylcobaloxime Complexes

Angela D. Follett, Katherine A. McNabb, Alicia A. Peterson, Joseph D. Scanlon, Christopher J. Cramer, and Kristopher McNeill*

Department of Chemistry and Supercomputing Institute, University of Minnesota, 207 Pleasant Street SE, Minneapolis, Minnesota 55455

Received September 26, 2006

This study combines theory and experiment in an examination of Co–C bonding and reductive Co–C cleavage in cobalt dichlorovinyl complexes. It is motivated by the role of dichlorovinyl complexes as intermediates in the dechlorination of trichloroethylene by cobalamin and cobalamin model complexes. A series of seven *cis*-1,2-dichlorovinyl(L)cobaloxime complexes were prepared (L = *m*- and *p*-substituted pyridines; cobaloxime = bis-(dimethylglyoximato)cobalt). The complexes were characterized using ^{1}H NMR, ^{13}C NMR, cyclic voltammetry, and X-ray crystallography. Examination of the metrical parameters of the Co–C═C unit across the series shows very little change in the C═C bond length and a slight increase in the Co–C bond length with increasing electron-donating ability of the pyridine ligand. These structural changes along with electronic structure calculations indicate that Co–C π-bonding is not important in these complexes. The stronger Co–C bonds of vinylcobaloximes compared to those of alkylcobaloximes are best explained by the higher s character at C. Changes in the reduction potential across the series indicate that the pyridine-bound form is the primary electrochemically active species. Theoretical examination of the Co–C cleavage following reduction supports the direct formation of the *cis*-1,2-dichlorovinyl anion and not the *cis*-1,2-dichlorovinyl radical.

Introduction

The cobalt−carbon bonds of alkylcobalt(III) complexes have been extensively studied due to their relevance to biologically important cofactors methylcobalamin and adenosylcobalamin.[1−9] These organometallic species are characterized by their low metal−carbon bond strength, which leads to facile thermal and photochemical homolytic cleavage.[10] Our research in the area of cobalt-mediated dechlorination reactions has drawn us to the less well-studied Co(III)−vinyl bonds and specifically to Co(III)−chlorovinyl bonds. This is because chlorovinylcobalt complexes are believed to be key intermediates in the dechlorination of chlorinated ethylenes promoted by cobalamin and other Co complexes.[11−25]

* To whom correspondence should be addressed. E-mail: mcneill@chem.umn.edu.

(1) Zhou, D. L.; Tinembart, O.; Scheffold, R.; Walder, L. *Helv. Chim. Acta* **1990**, *73*, 2225−2241.
(2) Bakac, A.; Espenson, J. H. *J. Am. Chem. Soc.* **1984**, *106*, 5197−5202.
(3) Tinembart, O.; Walder, L.; Scheffold, R. *Ber. Bunsen-Ges. Phys. Chem.* **1988**, *92*, 1225−1231.
(4) Chiu, P.-C.; Reinhard, M. *Environ. Sci. Technol.* **1996**, *30*, 1882−1889.
(5) Martin, B. D.; Finke, R. G. *J. Am. Chem. Soc.* **1992**, *114*, 585−592.
(6) Assaf-Anid, N.; Lin, K.-Y. *J. Environ. Eng.* **2002**, *128*, 94−99.
(7) Lexa, D.; Savéant, J.-M. *J. Am. Chem. Soc.* **1978**, *100*, 3220−3222.
(8) Schrauzer, G. N. *Angew. Chem., Int. Ed. Engl.* **1976**, *15*, 417−426.
(9) Argüello, J. E.; Costentin, C.; Griveau, S.; Savéant, J.-M. *J. Am. Chem. Soc.* **2005**, *127*, 5049−5055.
(10) Schrauzer, G. N.; Sibert, J. W.; Windgassen, R. J. *J. Am. Chem. Soc.* **1968**, *90*, 6681−6688.
(11) Glod, G.; Angst, W.; Holliger, C.; Schwarzenbach, R. P. *Environ. Sci. Technol.* **1997**, *31*, 253−260.
(12) Semadeni, M.; Chiu, P.-C.; Reinhard, M. *Environ. Sci. Technol.* **1998**, *32*, 1207−1213.
(13) Lesage, S.; Brown, S.; Millar, K. *Environ. Sci. Technol.* **1998**, *32*, 2264−2272.
(14) Burris, D. R.; Delcomyn, C. A.; Smith, M. H.; Roberts, A. L. *Environ. Sci. Technol.* **1996**, *30*, 3047−3052.
(15) Kim, Y. H.; Carraway, E. R. *Environ. Technol.* **2002**, *23*, 1135−1145.
(16) McCauley, K. M.; Wilson, S. R.; van der Donk, W. A. *Inorg. Chem.* **2002**, *41*, 393−404.
(17) McCauley, K. M.; Wilson, S. R.; van der Donk, W. A. *Inorg. Chem.* **2002**, *41*, 5844−5848.
(18) McCauley, K. M.; Wilson, S. R.; van der Donk, W. A. *J. Am. Chem. Soc.* **2003**, *125*, 4410−4411.
(19) McCauley, K. M.; Pratt, D. A.; Wilson, S. R.; Shey, J.; Burkey, T. J.; van der Donk, W. A. *J. Am. Chem. Soc.* **2005**, *127*, 1126−1136.
(20) Pratt, D. A.; van der Donk, W. A. *J. Am. Chem. Soc.* **2005**, *127*, 384−396.
(21) Pratt, D. A.; van der Donk, W. A. *Chem. Commun.* **2006**, 558−560.

10.1021/ic0618293 CCC: $37.00
Published on Web 02/08/2007

Scheme 1

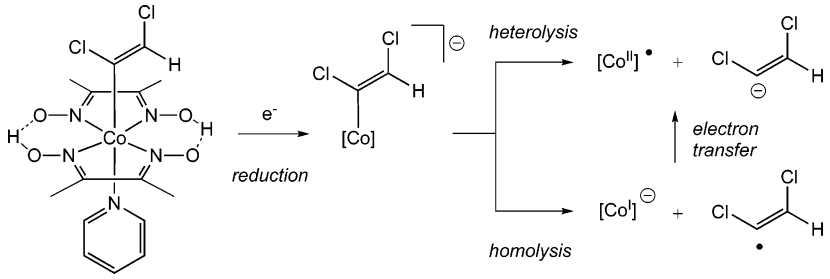

Compared to their alkyl analogues, cobalt−vinyl bonds are generally more robust toward homolysis. In line with this observation, Co−vinyl bond dissociation enthalpies have been calculated to be approximately 10 kcal/mol higher than those of Co−alkyl bonds.[20] The higher bond strength could be the result of improved σ bonding, a π-bonding contribution, or a combination of both σ and π effects. Enhanced σ bonding is expected due to the higher s character of the vinyl carbon compared to that of an alkyl carbon. It is less clear-cut whether there is any significant π-bonding, which could arise from metal-to-ligand back-bonding into the vinyl π system. The first goal of the work presented here is to determine whether π-bonding effects are important in the metal−carbon bonding of Co(III)−dichlorovinyl complexes. We have approached this question from two directions by looking at the variation in solid-state structure across a series of seven *cis*-1,2-dichlorovinyl(L)cobaloxime complexes (L = substituted pyridine) and by performing electronic structure calculations.

Under catalytic dechlorination conditions using cobalamin, reductive cleavage of the Co(III)−chlorovinyl bond is thought to be an important process that releases the vinyl group and allows for catalyst turnover. There has been an ongoing discussion of whether the vinyl group is released as a radical or an anion.[1,3,12,13,15,18,19,26] Good evidence for the intermediacy of radicals comes from experiments in which deuterium is incorporated in the dechlorination products when the catalytic dechlorination reaction is performed in the presence of weak C−D bonds of d_7-isopropyl alcohol.[11] In a cobalamin model system, we have recently obtained experimental evidence that supports formation of the *cis*-1,2-dichlorovinyl anion and not radical intermediates from reduction of *cis*-1,2-dichlorovinyl(pyridine)cobaloxime.[27] This observation is supported by calculations performed for the corresponding complexes in the cobalamin system.[20] Perhaps reconciling these disparate observations, Pratt and van der Donk have proposed that, in addition to chlorovinyl complexes, chloroalkyl complexes may be formed and serve as carbon-based radical precursors.[21]

While the evidence pointing to the formation of dichlorovinyl anions from reduced *cis*-1,2-dichlorovinyl(pyridine)-cobaloxime is strong, it is currently unclear whether the formation of the dichlorovinyl anion is the result of direct heterolytic cleavage of the cobalt−carbon bond or from homolytic cleavage followed by a fast in-cage electron transfer from Co^I to the vinyl radical (Scheme 1).[27] Analogous Co(III)−alkyl complexes offer little guidance on this point since reductive cleavage is known to produce both alkyl radicals and carbanion species.[3] Thus, a second goal of this work is to use theory to examine specifically whether reduced *cis*-1,2-dichlorovinyl(pyridine)cobaloxime decomposes directly to the *cis*-1,2-dichlorovinyl anion (heterolysis) or via a 1,2-dichlorovinyl radical intermediate (homolysis followed by electron transfer).

Experimental Section

General Methods. All NMR spectra were recorded on a Varian Inova 500 MHz spectrometer. High-resolution mass spectrometry (HRMS) measurements were made on a Bruker BioTOF II instrument under positive ionization mode. UV−vis absorbance spectra were obtained on an Ocean Optics CHEMUSB2 spectrophotometer. Infrared spectra were taken on a Midac M series spectrometer in methylene chloride. All reagents and solvents were purchased from commercial suppliers, unless otherwise stated. *N*,*N*-Dimethylformamide (DMF) was dried over 4 Å molecular sieves followed by distillation under reduced pressure prior to use.

***cis*-1,2-Dichlorovinyl(pyridine)cobaloxime (4).** Complex **4** was prepared by a procedure modified from Rich et al.[22] Cobalt(II) acetate tetrahydrate (0.500 g, 2.00 mmol) was combined with dimethylglyoxime (0.460 g, 4.00 mmol) and pyridine (0.460 mL, 5.72 mmol) in 50 mL of unstabilized THF under N_2. To this solution was added zinc powder (0.680 g, 10.5 mmol) under N_2 flow, and the solution was heated to 65 °C for 15 min. The solution was then cooled to room temperature, and trichloroethylene (TCE) (0.900 mL, 10.0 mmol) was added. The reaction mixture was again heated to 65 °C for 1 h. The reaction mixture was cooled to room temperature and filtered through Celite. The resulting red-orange solution was concentrated to a solid under vacuum. This material was chromatographed (SiO_2, THF), and the orange band was collected. The solvent was removed from this fraction in vacuo, and the yellow-orange residue was dissolved in $CHCl_3$. This solution was washed with H_2O (3 × 50 mL). The aqueous layers were combined and back-extracted with $CHCl_3$ (3 × 50 mL). The chloroform layers were combined, dried ($MgSO_4$), and filtered. The solvent was removed under vacuum. The yellow product was recrystallized from $CHCl_3$/hexanes (1:3), producing purified material in a 78% yield (0.725 g, 1.56 mmol) following recrystallization. The identity of the product was confirmed by its ^{1}H NMR spectrum.[16,17,22,27]

(22) Rich, A. E.; DeGreeff, A. D.; McNeill, K. *Chem. Commun*. **2002**, 234−235.
(23) Costentin, C.; Robert, M.; Savéant, J.-M. *J. Am. Chem. Soc*. **2005**, *127*, 12154−12155.
(24) Follett, A. D.; McNeill, K. *J. Am. Chem. Soc.* **2005**, *127*, 844−845.
(25) Fritsch, J. M.; McNeill, K. *Inorg. Chem.* **2005**, *44*, 4852−4861.
(26) Hogenkamp, H. P. C. In B_{12}; John Wiley & Sons: New York, 1982; Vol. 1, pp 295−323.
(27) Follett, A. D.; McNeill, K. *Inorg. Chem.* **2006**, *45*, 2727−2732.

***cis*-1,2-Dichlorovinyl(4-dimethylaminopyridine)cobaloxime (1).** Complex **1** was synthesized using the procedure described in the preceding section with 4-dimethylaminopyridine (0.740 g, 6.03 mmol) being used in place of pyridine. Yield: 42% (0.426 g, 0.840 mmol). ^{1}H NMR ($CDCl_3$): δ ppm 2.18 (12H, s, CH_3), 2.98 (6H, s, NCH_3), 5.74 (1H, s, CHCl), 6.38 (2H, d, J = 7.0 Hz, pyr), 7.96 (2H, d, J = 6.5 Hz, pyr). ^{13}C NMR ($CDCl_3$): δ ppm 12.56 (CH_3), 39.26 (NCH_3), 107.05 (CHCl), 107.84 (pyr), 148.89 (pyr), 150.66 (C═N), 154.57 (pyr). IR (cm^{-1}): 3019 (s), 2361 (w), 1623 (w), 1553 (w), 1428 (w), 1213 (s). HRMS: [M + Na$^+$] calcd for $C_{17}H_{25}Cl_2CoN_6O_4$, 529.0544; found, 529.0533.

***cis*-1,2-Dichlorovinyl(4-methoxypyridine)cobaloxime (2).** Preparation of **2** followed the general procedure outlined, replacing pyridine with 4-methoxypyridine (0.625 mL, 8.05 mmol). Yield: 35% (0.358 g 0.724 mmol) after recrystallization. ^{1}H NMR ($CDCl_3$): δ ppm 2.18 (12H, s, CH_3), 3.82 (3H, s, OCH_3), 5.75 (1H, s, CHCl), 6.78 (2H, d, J = 7.0 Hz, pyr), 8.30 (2H, d, J = 6.5 Hz, pyr). ^{13}C NMR ($CDCl_3$): δ ppm 12.70 (CH_3), 55.93 (OCH_3), 107.35 (CHCl), 111.82 (pyr), 151.25 (C═N and pyr), 167.13 (pyr). IR (cm^{-1}): 3020 (s), 1216 (s). HRMS: [M + Na$^+$] calcd for $C_{16}H_{22}Cl_2CoN_5O_5$, 516.0228; found, 516.0218.

***cis*-1,2-Dichlorovinyl(3,5-dimethylpyridine)cobaloxime (3).** Synthesis of **3** used a modified procedure for **4**, substituting 3,5-dimethylpyridine (0.690 mL, 6.05 mmol) for pyridine and using a solvent mixture of 1:1 THF/$CHCl_3$ with 1% triethylamine (NEt_3) for column chromatography. Recrystallization was performed by dissolving the solid in a minimal amount of $CHCl_3$ followed by slow diffusion of hexanes. A yield of 28% (0.271 g, 0.551 mmol) was obtained after recrystallization. ^{1}H NMR ($CDCl_3$): δ ppm 2.18 (12H, s, CH_3), 2.27 (6H, s, pyr CH_3), 5.76 (1H, s, CHCl), 7.33 (1H, s, pyr), 8.14 (2H, s, pyr). ^{13}C NMR ($CDCl_3$): δ ppm 12.71 (CH_3), 18.80 (pyr CH_3), 107.32 (CHCl), 135.09 (pyr), 140.02 (pyr), 147.44 (pyr), 151.10 (C═N). IR (cm^{-1}): 3018 (w), 2361 (b), 1216 (s). HRMS: [M + Na$^+$] calcd for $C_{17}H_{24}Cl_2CoN_5O_4$, 514.0435; found, 514.0443.

***cis*-1,2-Dichlorovinyl(3-methoxypyridine)cobaloxime (5).** Complex **5** was prepared by an analogous reaction to that used previously for **4**, replacing the pyridine with 3-methoxypyridine (0.500 mL, 4.92 mmol) and starting with 400 mg of $Co(OAc)_2{\cdot}4H_2O$ (1.61 mmol). The solid was recrystallized by slow evaporation of THF, producing a yield of 35% (0.278 g, 0.562 mmol). ^{1}H NMR ($CDCl_3$): δ ppm 2.18 (12H, s, CH_3), 3.81 (3H, s, OCH_3), 5.76 (1H, s, CHCl), 7.23 (2H, m, pyr), 8.15 (1H, dd, J = 1.0, 5.5 Hz, pyr), 8.24 (1H, d, J = 3.0 Hz, pyr). ^{13}C NMR ($CDCl_3$): δ ppm 12.72 (CH_3), 56.12 (OCH_3), 107.37 (CHCl), 123.49 (pyr), 125.57 (pyr), 137.82 (pyr), 142.62 (pyr), 151.30 (C═N), 156.86 (pyr). IR (cm^{-1}): 3020 (s), 2361 (b), 1216 (s). HRMS: [M + H$^+$] calcd for $C_{16}H_{22}Cl_2CoN_5O_5$, 494.0408; [M + Na$^+$] found, 494.0398.

***cis*-1,2-Dichlorovinyl(3-acetylpyridine)cobaloxime (6).** Preparation of compound **6** followed the preparation of **4**, substituting 3-acetylpyridine (0.660 mL, 4.95 mmol) for pyridine. The yield following recrystallization was 32% (0.320 g, 0.653 mmol). ^{1}H NMR ($CDCl_3$): δ ppm 2.19 (12H, s, CH_3), 2.61 (3H, s, $COCH_3$), 5.76 (1H, s, CHCl), 7.47 (1H, dd, J = 6.0, 10.0 Hz, pyr), 8.29 (1H, dt, J = 2.0, 7.5 Hz, pyr), 8.70 (1H, dd, J = 1.0, 5.5 Hz, pyr), 9.11 (1H, d, J = 1.5 Hz, pyr). ^{13}C NMR ($CDCl_3$): δ ppm 12.79 (CH_3), 26.97 ($COCH_3$), 107.57 (CHCl), 125.89 (pyr), 134.34 (pyr), 137.69 (pyr), 150.84 (pyr), 151.70 (C═N), 153.83 (pyr), 194.86 (pyr). IR (cm^{-1}): 3019 (s), 2433 (w), 1520 (b), 1439 (w), 1213 (s). HRMS: [M + Na$^+$] calcd for $C_{17}H_{22}Cl_2CoN_5O_5$, 528.0228; found, 528.0234.

***cis*-1,2-Dichlorovinyl(4-cyanopyridine)cobaloxime (7).** Complex **7** was synthesized using a modified procedure for **4**, substituting 4-cyanopyridine (0.620 g, 6.00 mmol) for pyridine. Yield: 25% (0.245 g, 0.501 mmol) following recrystallization. ^{1}H NMR ($CDCl_3$): δ ppm 2.18 (12H, s, CH_3), 5.75 (1H, s, CHCl), 7.57 (2H, d, J = 6.5 Hz, pyr), 8.79 (2H, d, J = 6.5 Hz, pyr). ^{13}C NMR ($CDCl_3$): δ ppm 12.85 (CH_3), 107.77 (CHCl), 111.79 (cyano), 115.16 (pyr), 123.17 (pyr), 151.08 (pyr), 151.17 (C═N). IR (cm^{-1}): 3020 (s), 2497 (w), 1214 (s). HRMS: [M + Na$^+$] calcd for $C_{16}H_{19}Cl_2CoN_6O_4$, 511.0075; found, 510.9988.

X-ray Structure Determination. Diffraction data for complexes **1**−**7**, mounted on thin glass capillaries with oil, were collected on a Bruker or Siemens SMART Platform CCD diffractometer with Mo Kα radiation (graphite monochromator) at 173(2) K. Structures were solved using SHELXS-97 and were refined using SHELXL-97.[28] Crystallographic data for all of the structures are summarized in Table 1. All of the structures contained cocrystallized solvent. Compound **5** contained THF, and all other complexes contained $CHCl_3$, which was disordered over two or more positions but was modeled effectively.

Complex **1** was on a special position, a mirror plane that contains the vinyl and dimethylaminopyridine ligands and reflects the two dimethylglyoxime ligands onto each other. The hydroxyl hydrogen atoms were set to a 50:50 residence time on either side of the mirror plane.

Compound **2** showed nonmerohedral twinning with a ratio of twin components of 59:41; the molecule lies on a pseudo-mirror plane, and there is a pseudo b glide in the unit cell.

The single-crystal X-ray structure of compound **4** has been determined twice before in two different crystal systems (*P*1 as a $CHCl_3$ solvate and *C*2/*c* as a CH_2Cl_2 solvate).[16,29] Because the bond lengths between the two structures were not in good agreement, we performed a third crystal structure. In the present case, the compound crystallized as a $CHCl_3$ solvate in *P*1 with the same unit cell parameters found by Jones et al. As Jones et al. point out, *P*1 is an unusual space group for a racemate, but we agree that the space group assignment is correct. The crystal was a racemic twin (68:32). In addition, the dichlorovinyl group was disordered and was effectively modeled over two positions with a ratio of 77:23. None of the structures of **4** appear to be definitive, as there are significant metrical discrepancies between all three. For example, the Co−C bond lengths found by McCauley et al., Jones et al., and in this study are 1.945(5), 1.958(3), and 1.950(8) Å, respectively. The C═C bond lengths of the vinyl ligand are 1.32(3), 1.324(3), and 1.247(16) Å.

Compound **6** was a pseudomerohedral twinned structure with a ratio of 97:3.

Electrochemistry. Cyclic voltammetry (CV) experiments were conducted using a BAS 100B electrochemical analyzer with a normal three-electrode configuration consisting of a Pt auxiliary electrode, a highly polished glassy carbon working electrode (A = 0.07 cm^2), and a Ag$^+$/AgCl reference electrode containing 1.0 M KCl. The 5 mL working compartment was separated from the reference compartment by a modified Luggin capillary. All three compartments were filled with a solution of dry DMF containing 0.1 M tetrabutylammonium hexafluorophosphate ($TBAPF_6$) as the supporting electrolyte. In all of the experiments, the working compartments of the cell were bubbled with argon to deaerate the solution. Solutions were prepared by recording the background cyclic voltammograms of the electrolyte solution prior to addition of a solid sample. The potentials are reported versus Ag$^+$/AgCl

(28) *SHELXTL*, V6.14; Bruker Analytical X-ray Systems: Madison, WI, 2000.
(29) Jones, P. G.; Yang, L.; Steinborn, D. *Acta Crystallogr., Sect. C* **1996**, *52*, 2399−2402.

Table 1. Crystallographic Data for Compounds **1**−**7**

compound	**1**	**2**	**3**	**4**	**5**	**6**	**7**
formula	$C_{17}H_{25}Cl_2CoN_6O_4$	$C_{16}H_{22}Cl_2CoN_5O_5$	$C_{17}H_{24}Cl_2CoN_5O_4$	$C_{15}H_{21}Cl_2CoN_5O_4$	$C_{16}H_{22}Cl_2CoN_5O_5$	$C_{17}H_{22}Cl_2CoN_5O_5$	$C_{16}H_{19}Cl_2CoN_6O_4$
habit	plate	plates	block	needle	block	block	block
color	yellow	yellow	orange	orange	orange	orange	orange
lattice type	monoclinic	monoclinic	monoclinic	triclinic	orthorhombic	monoclinic	monoclinic
space group	$P2_1/m$	$P2_1/n$	$P2_1/n$	$P1$	$P2_12_12_1$	$P2_1/c$	$P2_1/n$
a, Å	9.1043(18)	9.048(2)	8.6608(5)	8.1545(6)	8.7827(6)	8.8740(18)	13.5768(14)
b, Å	14.307(3)	22.314(6)	13.8210(9)	8.8842(7)	15.1091(11)	16.515(3)	13.5270(14)
c, Å	12.143(2)	14.317(4)	21.7552(14)	8.9348(8)	21.9839(16)	17.328(4)	14.4196(15)
α deg	90	90	90	82.507(3)	90	90	90
β deg	102.144(3)	90.766	95.2590(10)	89.493(3)	90	90.176(4)	107.801(2)
γ deg	90	90	90	63.383(2)	90	90	90
V, Å^3	1546.3(5)	2890.6(13)	2593.2(3)	572.85(8)	2917.2(4)	2539.5(9)	2521.4(5)
Z	2	4	4	1	4	4	4
fw g mol^{-1}	507.26	494.22	492.24	464.18	494.22	506.23	489.20
D_c g cm^{-3}	1.602	1.684	1.567	1.692	1.454	1.636	1.603
μ, mm^{-1}	1.283	1.372	1.211	1.366	0.821	1.241	1.246
F(000)	756	1480	1248	296	1336	1272	1232
θ range deg	1.72 to 25.05	1.69 to 27.51	1.75 to 25.05	2.30 to 25.08	1.64 to 27.52	1.18 to 25.06	1.80 to 27.51
reflns collected	14647	6593	25673	5724	33997	25249	29297
unique reflns	2857	6593	4604	3981	6661	4516	5798
max, min transmission	1.0000, 0.8250	0.762, 0.729	1.0000, 0.8353	0.8755, 0.6464	1.0000, 0.8212	0.8859, 0.7893	0.6494, 0.5859
data/ restraint/ parameters	2857/10/237	6593/60/396	4604/24/326	3981/34/ 335	6661/0/357	4516/6/326	5798/6/315
R1	0.0637,	0.0676,	0.0344,	0.0355,	0.0319,	0.0312,	0.0384,
wR2 ($I > 2\sigma(I)$)	0.1520	0.2218	0.0911	0.0777	0.0736	0.0653	0.1027
R1,	0.0698,	0.0789,	0.0399,	0.0382,	0.0516,	0.0369,	0.0463,
wR2 (all data)	0.1559	0.2321	0.0953	0.0791	0.0798	0.0677	0.1076
GOF	1.044	1.060	1.071	1.030	0.946	1.031	1.031
largest diff peak, hole, e Å^{-3}	1.161, −1.073	1.186, −1.068	0.428, −0.381	0.500, −0.489	0.304, −0.260	0.337, −0.320	1.152, −0.760

and are not corrected for the junction potential. The $E^{\circ\prime}$ value for the ferrocenium/ferrocene couple under the conditions used in this study was +0.42 V. As the oxidation and reduction processes of compounds **1**−**7** are irreversible, regardless of the scan rate used (50−2000 mV/s), the reported values are given as the peak potentials. As these potentials, in general, depend on the concentration and scan rate, all voltammograms were measured at similar concentrations (0.48−0.52 mM) and scan rates (100 mV/s) to allow for reliable comparisons of their potentials.

Theoretical Methods. All structures were optimized with the hybrid density functional B3LYP[30−33] using the Gaussian98[34] and Gaussian03 version d01[35] suites of electronic structure programs. For gas-phase calculations, the 6-31+Gd basis set[36] was used for all nonmetal atoms and the Stuttgart basis set and effective core potential[37] for cobalt. To account for solvation effects, single-point calculations on the gas-phase minima were performed using the implicit solvation model SM5.43R[38] for DMSO, as implemented in MN-GSM.[39] For the single-point solvation calculations, a smaller basis set, 6-31Gd, was used for all nonmetal atoms, and a Coulomb radius of 2 Å was employed for cobalt. To examine reaction coordinates corresponding to Co−C_α bond dissociation, these bonds were incrementally stretched from their equilibrium positions, and remaining structural degrees of freedom were then allowed to relax in the gas phase. Single-point solvation calculations were performed on the relaxed structures to evaluate the influence of the condensed phase on the electronic structures. Bond energies computed as differences between complexes and separated constituents were corrected for basis set superposition error (BSSE) using standard counterpoise procedures.[40]

(30) Becke, A. D. *J. Chem. Phys.* **1993**, *98*, 5648−5652.
(31) Becke, A. D. *Phys. Rev. A* **1988**, *38*, 3098−3100.
(32) Lee, C. T.; Yang, W. T.; Parr, R. G. *Phys. Rev. B* **1988**, *37*, 785−789.
(33) Stephens, P. J.; Devlin, F. J.; Chabalowski, C. F.; Frisch, M. J. *J. Phys. Chem.* **1994**, *98*, 11623−11627.
(34) Frisch, M. J.; Trucks, G. W.; Head-Gorden, M.; Gill, P. M. W.; Wong, M. W.; Foresman, J. B.; Johnson, B. G.; Schlegel, H. B.; Robb, M. A.; Replogle, E. S.; Gomperts, R.; Andres, J. L.; Rahavachari, K.; Binkley, J. S.; Gonzalez, C.; Martin, R. L.; Fox, D. J.; Defrees, D. J.; Baker, J.; Stewart, J. J. P.; Pople, J. A. *Gaussian 92*; Gaussian, Inc.: Pittsburgh, PA, 1992.
(35) Frisch, M. J.; Trucks, G. W.; Schlegel, H. B.; Scuseria, G. E.; Robb, M. A.; Cheeseman, J. R.; Montgomery, J. A., Jr.; Vreven, T.; Kudin, K. N.; Burant, J. C.; Millam, J. M.; Iyengar, S. S.; Tomasi, J.; Barone, V.; Mennucci, B.; Cossi, M.; Scalmani, G.; Rega, N.; Petersson, G. A.; Nakatsuji, H.; Hada, M.; Ehara, M.; Toyota, K.; Fukuda, R.; Hasegawa, J.; Ishida, M.; Nakajima, T.; Honda, Y.; Kitao, O.; Nakai, H.; Klene, M.; Li, X.; Knox, J. E.; Hratchian, H. P.; Cross, J. B.; Bakken, V.; Adamo, C.; Jaramillo, J.; Gomperts, R.; Stratmann, R. E.; Yazyev, O.; Austin, A. J.; Cammi, R.; Pomelli, C.; Ochterski, J. W.; Ayala, P. Y.; Morokuma, K.; Voth, G. A.; Salvador, P.; Dannenberg, J. J.; Zakrzewski, V. G.; Dapprich, S.; Daniels, A. D.; Strain, M. C.; Farkas, O.; Malick, D. K.; Rabuck, A. D.; Raghavachari, K.; Foresman, J. B.; Ortiz, J. V.; Cui, Q.; Baboul, A. G.; Clifford, S.; Cioslowski, J.; Stefanov, B. B.; Liu, G.; Liashenko, A.; Piskorz, P.; Komaromi, I.; Martin, R. L.; Fox, D. J.; Keith, T.; Al-Laham, M. A.; Peng, C. Y.; Nanayakkara, A.; Challacombe, M.; Gill, P. M. W.; Johnson, B.; Chen, W.; Wong, M. W.; Gonzalez, C.; Pople, J. A. *Gaussian 03*, revision C.02; Gaussian, Inc.: Wallingford, CT, 2004.
(36) Hehre, W. J.; Radom, L.; Schleyer, P. v. R.; Pople, J. A. *Ab Initio Molecular Orbital Theory*; Wiley: New York, 1986.
(37) Dolg, M.; Wedig, U.; Stoll, H.; Preuss, H. *J. Chem. Phys.* **1987**, *86*, 866−872.
(38) Thompson, J. D.; Cramer, C. J.; Truhlar, D. G. *Theor. Chem. Acc.* **2005**, *113*, 107−131.

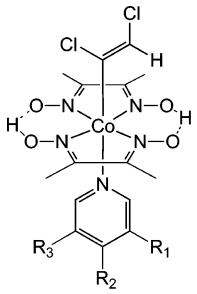

	R_1	R_2	R_3
1	H	$N(CH_3)_2$	H
2	H	OCH_3	H
3	CH_3	H	CH_3
4	H	H	H
5	OCH_3	H	H
6	Ac	H	H
7	H	CN	H

Figure 1. Structures and numbering of the series of *cis*-1,2-dichlorovinylcobaloximes prepared and characterized in this study.

We note that **4** has been previously studied by Rovira et al. in both the gas phase and in the crystalline solid state.[41] While Rovira et al. did not report gas-phase structures, nor did they report the density functional model used to optimize these structures, they did note dynamic behavior of the protons in the glyoximate ligands, such that structures with both acidic protons localized to one glyoxime ligand were observed in solid-state simulations. In the gas phase, they noted that such a proton-transfer structure constituted a second local minimum 2 kcal mol^{-1} higher in energy than the normal tautomer. We also located the proton-transfer tautomer in selected instances for **1**−**7**, and we found it to be stationary and higher in energy than the normal tautomer by similar margins of energy. Structural and energetic changes associated with the proton transfer were observed to be quite small and did not affect any of the qualitative trends displayed by the normal tautomers. On that basis, we henceforth discuss only data associated with the normal tautomer.

Results and Discussion

Synthesis and Characterization. A series of *cis*-1,2-dichlorovinyl(L)cobaloxime complexes were prepared, where L represents a meta- or para-substituted pyridine ligand. The parent compound, where L is pyridine, has been prepared previously,[16,17,22,27] and the method of Rich et al. was modified and used to synthesize the compounds in this study (Figure 1).[22] Briefly, the compounds were prepared by the following reaction protocol. Cobalt acetate tetrahydrate, dimethylglyoxime (dmgH), zinc powder, and the substituted pyridine were reacted at 65 °C for 15 min, presumably forming a cob(I)aloxime anion, $(dmgH)_2Co^-$, in situ. The dichlorovinyl complex was formed following addition of trichloroethylene (TCE) and heating to 65 °C for 1 h. In all cases, this crude reaction extract required further purification by column chromatography, aqueous workup, and recrystallization. All complexes were characterized by ^1H and ^{13}C NMR spectroscopy, high-resolution mass spectrometry (HRMS), and X-ray structure analysis.

X-ray Characterization. Structural characterization and the stereochemistry of compounds **1**−**7** was further confirmed through X-ray crystallography. Crystal structures of each of the complexes were obtained (Figure 2). In all cases, the chlorovinyl group and the pyridine ligand were aligned in the same plane and were situated over the bridging oxygen atoms of the equatorial dimethylglyoxime ligands. This orientation is consistent with that observed with other chlorovinyl and vinylcobaloxime structures, with the exception of *cis*-chlorovinylcobaloxime, which contains a sterically strained chlorovinyl species.[16,17,29]

Table 2 contains selected bond lengths and angles for compounds **1**−**7** found in this study as well as those for previous structures of *cis*-1,2-dichlorovinyl(pyridine)cobaloxime (**4**),[16,29] vinyl(pyridine)cobaloxime (**8**),[16] and methyl(pyridine)cobaloxime (**9**),[42] shown for comparison. The Co−C bond lengths of the dichlorovinyl complexes, which ranged from 1.944 to 1.958 Å, all fell within the range observed for other vinylcobaloximes and were shorter than that observed in methylcobaloxime, **9**. The $Co-N_5$ bond lengths were also distributed in a range comparable to previously observed species.

The presence of an apparent preferred orientation of the axial ligands in the solid-state structures of complexes **1**−**7** is suggestive of π-bonding. As mentioned above, this might be expected since the dichlorovinyl ligand has available π orbitals that could be used in metal-to-ligand π back-bonding. A more in depth analysis of the structures, however, indicates that σ bonding is the dominant factor in cobalt−carbon bonding.

Examination of the bond lengths within the series reveals a relationship between the Hammett substituent constant (σ) and the length of the $Co-C_\alpha$ bond (Figure 3). The overall change in the bond length between the complexes is small (0.014 Å), but a general lengthening trend is observed with an increase in the electron-donating ability of the axial pyridine ligand; this trend is also found in our theoretical structures, although in the gas phase, the total variation is predicted to be only 0.007 Å. Increased π back-bonding to the vinyl group associated with a more-donating *trans*-pyridine ligand would be expected to decrease the $Co-C_\alpha$ bond length (Figure 4). In this study, we found the opposite trend; the $Co-C_\alpha$ bond length increases with increasing electronic donation from the pyridine ligand. Such behavior is more consistent with a standard *trans* influence trend. The weak sensitivity of the $Co-C_\alpha$ bond lengths to variations in *trans* substituents has been noted previously in model cobalamins.[43] Of course, there could be a back-bonding contribution, and its effect is not seen in the $Co-C_\alpha$ bond length because it is masked by the *trans* influence. We do not believe this to be the case, based on the analysis of other metrical parameters and on our theoretical results.

As a separate geometric analysis, if π back-bonding were important, lengthening of the vinyl C═C bond would be expected with increasing π-donating ability of the *trans* ligand (Figure 4). However, we observe no relationship between the length of the $\alpha-\beta$ carbon−carbon bond of the dichlorovinyl group and the Hammett substituent constant

(39) Chamberlin, A. C.; Kelly, C. P.; Thompson, J. D.; Xidos, J. D.; Li, J.; Hawkins, G. D.; Winget, P. D.; Zhu, T.; Rinaldi, D.; Liotard, D. A.; Cramer, C. J.; Truhlar, D. G.; Frisch, M. J. *MN-GSM*, Version 6.0; University of Minnesota: Minneapolis, MN, 2006.
(40) Cramer, C. J. *Essentials of Computational Chemistry*, 2nd ed.; Wiley: Chichester, U.K., 2004; pp 195−196.
(41) Rovira, C.; Kune, K.; Parrinello, M. *Inorg. Chem.* **2002**, *41*, 4810−4814.
(42) Bigotto, A.; Zangrando, E.; Randaccio, L. *J. Chem. Soc., Dalton Trans.* **1976**, 96−104.
(43) Andruniow, T.; Zgierski, M. Z.; Kozlowski, P. M. *J. Phys. Chem. B* **2000**, *104*, 10921−10927.

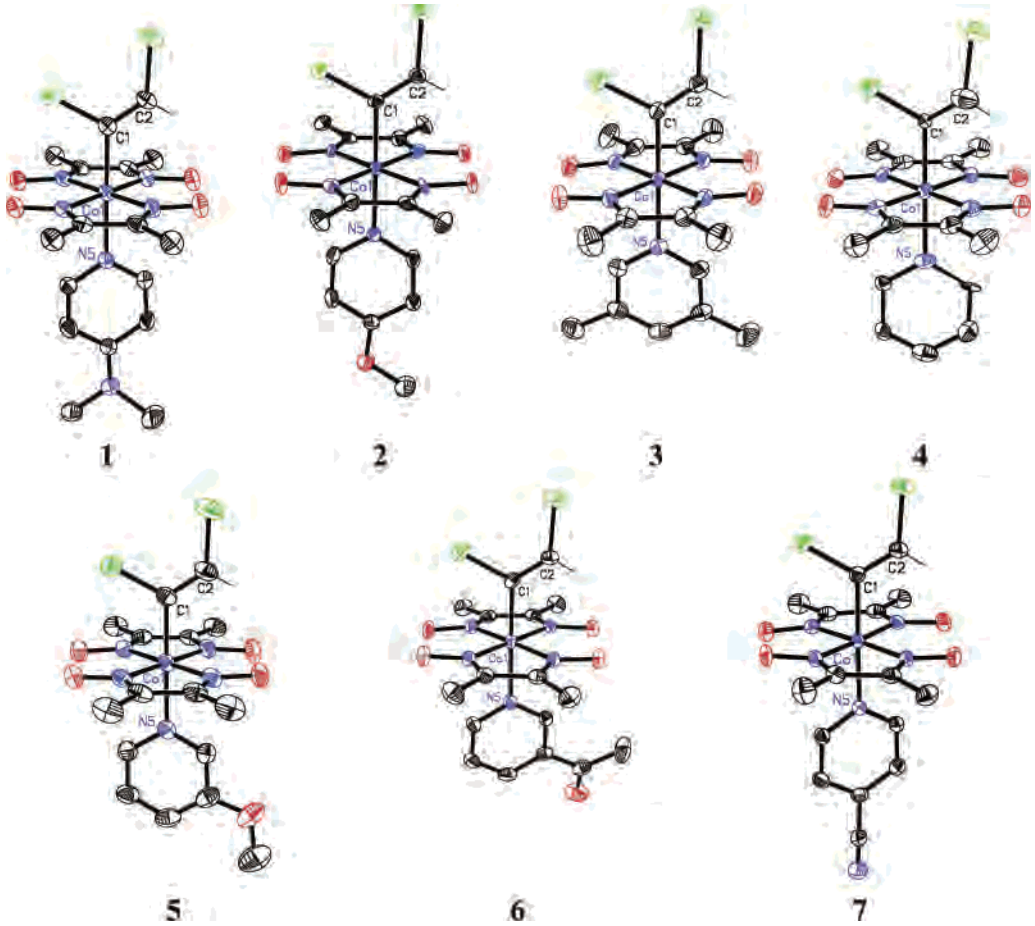

Figure 2. ORTEP diagrams of complexes **1**−**7**. Hydrogens, except for the chlorovinyl hydrogen, have been omitted for clarity; only the main position of the dichlorovinyl is depicted for complex **4**. The ellipsoids are shown at the 50% probability level.

Table 2. Selected Bond Lengths (Å) and Angles (deg) for Complexes **1**−**7** and Reference Compounds **8** and **9**[a]

	Co−C_1	Co−N_5	C_1−C_2	Co−C_1−C_2	C_1−Co−N_5	ref
1	1.958(6)	2.013(6)	1.315(9)	124.3(5)	177.2(5)	*b*
2	1.955(4)	2.027(4)	1.335(6)	122.5(3)	178.94(19)	*b*
3	1.953(2)	2.038(2)	1.324(3)	123.4(2)	179.55(10)	*b*
4	1.950(8)	2.030(4)	1.247(16)	120.8(12)	179.1(3)	*b*
	1.945(4)	2.030(2)	1.32(3)	121(2)	178.5(11)	16
	1.958(3)	2.028(2)	1.324(7)	123.3(3)	179.01(14)	29
5	1.952(2)	2.0341(19)	1.316(3)	124.04(18)	179.43(9)	*b*
6	1.951(2)	2.0337(19)	1.314(3)	123.16(18)	178.00(9)	*b*
7	1.944(2)	2.0353(18)	1.326(3)	122.16(17)	178.74(8)	*b*
8	1.953(3)	2.0518(15)	1.292(4)	127.8(3)	175.51(12)	16
9	1.998(5)	2.068(3)	−	−	178.0(2)	42

[a] C_1 and C_2 correspond to C_α and C_β in the text. Esds are shown in parentheses. [b] This work.

(Table 2). It is interesting to note that another metric, the Co−C−C bond angle, is a poor measure of hybridization of the carbon atom bound to Co. This can be seen in the fact that the Co−C−C linkage in sp^3-hybridized adenosylcobalamin has essentially the same 123° angle found for the sp^2-hybridized dichlorovinylcobaloximes in this study.[44,45]

In prior studies, the optical spectra of complexes have proven useful in elucidating the nature of the bonding, especially with respect to involvement of the metal d orbitals.

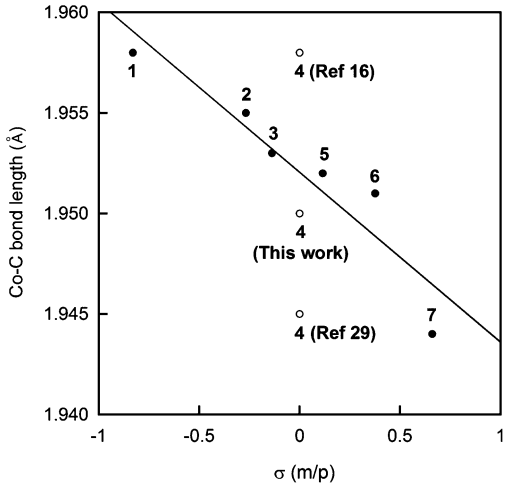

Figure 3. Observed relationship between the Co−C_α bond length and the Hammett substitution constant of compounds **1**−**7**, as fit to a linear function ($m = 8.45 \times 10^{-3}$ Å/σ unit, $b = 1.952$ Å, $R^2 = 0.88$). Note that none of the values for the Co−C_α bond length found for compound **4** are used in the regression, as we believe that there are problems with all of the structures of **4**. See the Experimental Section for more detail on the three structure determinations of **4**.

Similar comparisons are difficult in the cobaloxime systems, however, as the d−d transitions for these complexes are obscured by an intense charge-transfer band.[46,47]

(44) Ouyang, L.; Rulis, P.; Ching, W. Y.; Nardin, G.; Randaccio, L. *Inorg. Chem.* **2004**, *43*, 1235−1241.
(45) We thank a reviewer for pointing this out.
(46) Schrauzer, G. N.; Lee, L.-P.; Sibert, J. W. *J. Am. Chem. Soc.* **1970**, *92*, 2997−3005.

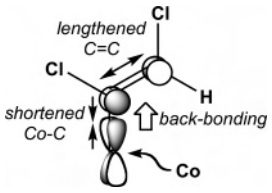

Figure 4. Expected effects of π back-bonding on the length of the Co−C_α and C_α−C_β bonds.

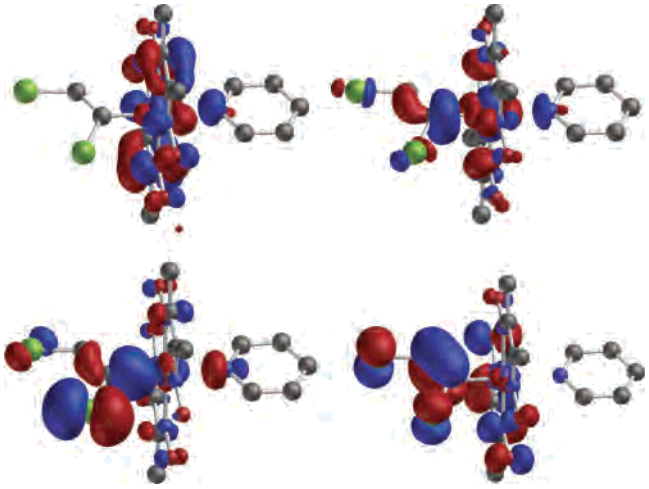

Figure 5. B3LYP HOMO−4 (lower left), HOMO−2 (lower right), LUMO (upper left), and LUMO+4 (upper right) orbitals for **4** depicted at the 0.04 au contour level; H atoms have been removed for clarity.

Insights into Bonding from Theory. Inspection of the molecular orbital (MO) shapes and energies for species **1**−**7** and their vinyl, **8**, and methyl, **9**, analogues suggests that the Co−C_α bond has almost entirely σ character, although the strength of the bond is subject to inductive effects associated with, for example, the chlorine substituents in the dichlorovinyl case. Particularly relevant MOs for **4** are illustrated in Figure 5. The highest occupied MO (HOMO) and HOMO−1 orbitals are π orbitals predominantly associated with the glyoxime ligands and are not shown. The HOMO−2 is a π orbital associated with the vinyl system (Figure 5). It is bonding across the C═C bond and includes substantial contributions from conjugating Cl atom lone pairs, but it has essentially no amplitude on the Co atom. An orbital corresponding to the back-bonding situation illustrated in Figure 4 is not present in the filled orbital manifold, nor within the first five virtual orbitals. Instead, MOs containing significant contributions from the relevant Co d orbital are found to be relatively low-energy π orbitals of the combined metal−glyoximate system. This is not particularly surprising, given that the glyoxime ligands are more electron rich than the dichlorovinyl species, have excellent overlap with the relevant Co d orbital, owing to short Co−N bond distances, and have occupied levels that are energy-matched better for hybridization with the d orbital compared to the halogen-substituted ethylene fragment.

The HOMO−3 is again associated with the glyoxime ligands (not shown), while the HOMO−4 is the Co−C_α σ bond (Figure 5). The contribution of Cl atomic orbitals to the MO is consistent with the inductive effect manifested by these electronegative halogen substituents.

As an alternative measure of π character in the Co−C_α bond, we examined the rotational barrier about this bond. Rotation of the vinyl unit, so as to place it perpendicular to the plane defined by the atoms of the pyridine ligand, led to a transition-state structure computed to be slightly less than 4 kcal mol^{-1} above the minimum. As this barrier is computed to be quite small and as π back-bonding might be expected to lead to a 4-fold symmetric potential instead of a 2-fold one, it would appear that this barrier is associated with only very weak steric and electronic interactions between the dichlorovinyl unit and the glyoximate ligands, and π back-bonding has little or no influence.

With respect to the virtual orbitals, the lowest occupied MO (LUMO), which initially becomes occupied following one-electron reduction, is a π^* orbital primarily associated with the glyoxime ligand; some small participation of the pyridine N lone pair (in an antibonding fashion) is also predicted (Figure 5). The LUMO+2 is also primarily a glyoxime π^* orbital, while LUMO+1 and LUMO+3 are both pyridine π^* orbitals. The Co−C_α σ^*, which is the orbital that must become populated along the bond dissociation coordinate, is found at LUMO+4. The energy of this orbital fluctuates with vibration of the Co−C_α bond; as the bond stretches, the orbital energy drops, making it more likely that electronic charge redistribution and subsequent bond scission may occur. In addition, the energy level is affected by the chlorine substituents in the dichlorovinyl case. Thus, while the Co−C_α σ^* orbital has an energy 0.031 au above the LUMO in vinyl complex **8**, that separation increases to 0.055 au in the dichlorovinyl complex, **4**.

In a particularly relevant study, Pratt and van der Donk examined virtual orbital energies in vinylcobalt(III) species supported by a corrin ligand and further coordinated by imidazole.[20] Similar to the situation observed here, the LUMO of their species was associated with the π system of the corrin when the imidazole base was present. However, they noted that, when the base was removed, the energy of the Co−C_α σ^* orbital dropped significantly so that this orbital became the new LUMO. This is consistent with a change from a 3-center, 4-electron bonding situation in the base-on form to a 2-center, 2-electron bonding situation in the base-off form. On the basis of comparison to experimental CV spectra showing different reduction potentials depending on scan speed for an analogous compound, Pratt and van der Donk suggested that an equilibrium between the base-on and base-off congeners might be rapid enough that reduction would occur primarily via the latter species, for which they computed reduction potentials more positive than those for base-on species by 710−1150 mV when dichloro- and trichlorovinyl ligands were involved.

We examined the effect of removing the pyridine base in our computational model. Like Pratt and van der Donk, we found the LUMO of the base-off system to be the Co−C_α σ^* orbital. However, under our experimental conditions, it is clear that reduction takes place primarily for the base-on species since the reduction potential is sensitive to substitu-

(47) Trogler, W. C.; Stewart, R. C.; Epps, L. A.; Marzilli, L. G. *Inorg. Chem.* **1974**, *13*, 1564−1570.

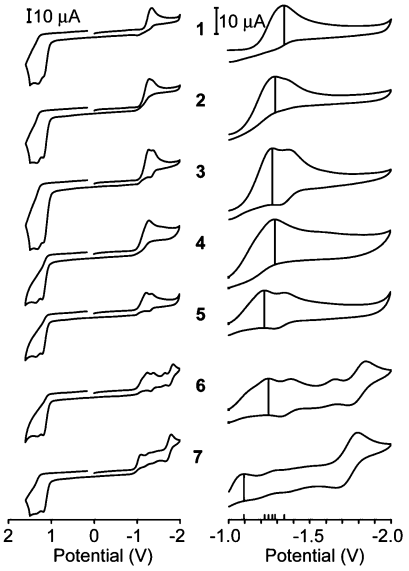

Figure 6. Voltammograms of complexes **1**−**7** at concentrations ranging from 0.48 to 0.52 mM in dry DMF. Potentials are reported as peak potential versus Ag^+/AgCl, with a sweep rate of 100 mV/s, using a glassy carbon electrode and 0.1 M $TBAPF_6$.

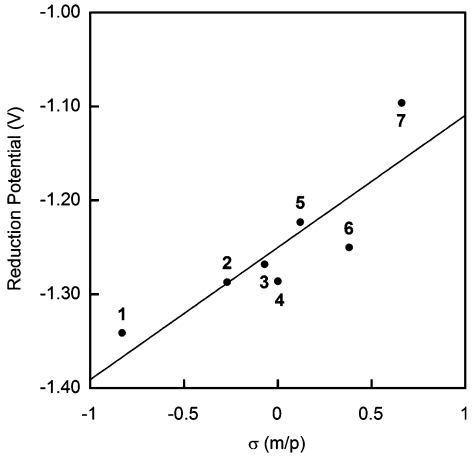

Figure 7. Free-energy relationship observed between the reduction potential for compounds **1**−**7** and the respective Hammett substituent constants (σ) of their axial pyridine. Potentials are reported as peak potential versus Ag^+/AgCl, with a sweep rate of 100 mV/s, using a glassy carbon electrode and 0.1 M $TBAPF_6$. The solid line is a linear least-squares fit to the data ($m = 0.14$ V/σ unit, $b = -1.25$ V, $R^2 = 0.76$).

tion of the pyridine ring. Nevertheless, it is likely a general phenomenon that analogous Co(III)alkyl and -vinyl species may have coupled complexation and electrochemical equilibria, and careful attention should be paid to this possibility.

Electrochemistry. Cyclic voltammetry was used to evaluate the redox properties of this series of complexes. Of particular interest was whether changes would be observed across the series, as it has been noted that, in the cobalamin system, the base-off form is likely to be the electrochemically active species.[20] In our study, **1**−**7** all share the same base-off form, the $(dmgH)_2Co(cis\text{-}CCl{=}CHCl)$ fragment. Voltammograms were measured for complexes **1**−**7** at concentrations ranging from 0.48 to 0.52 mM in dry DMF. Voltammograms for complexes **1**−**7** are shown in Figure 6. In all cases, the reduction was found to be completely irreversible up to a scan rate of 2 V/s, and no pyridine dissociation was observed prior to the reduction event. The irreversibility of electrochemical reduction is characteristic of chlorovinylcobaloximes, including compound **4**, and organocobalamins that have been previously reported.[9,16,18,23,48] The absence of an oxidation peak necessitated the use of the peak potential as the value for the overall reduction potential of the complexes. McCauley et al. found a peak potential of -1.13 ± 0.03 V for a 1 mM solution of **4** in 1:1 DMF/*t*BuOH versus Ag^+/AgCl at 100 mV/s.[16] In this work, for a 0.5 mM solution of **4** in dry DMF, we found a peak potential of -1.29 ± 0.05 V versus Ag^+/AgCl at the same scan rate.

Peak potentials for complexes **1**−**7** at 100 mV/s versus Ag^+/AgCl ranged from -1.10 to -1.34 V. Evaluating this value as a function of electron-donating ability of the pyridine produced a rough, linear free-energy relationship (Figure 7). As the electron-donating ability of the axial ligand was increased, a corresponding decrease in the reduction potential was observed. These results indicate that, in this series, the pyridine-bound form is the one that undergoes reduction.

Insights into Reduction from Theory. There is a fair to good correlation (Pearson correlation coefficient $R = 0.89$) between calculated, vertical, gas-phase electron affinities (EAs) and the experimental reduction potentials for compounds **1**−**7** (a similar correlation was observed with computed LUMO energies). As expected, as the electron-donating capability of the para-substituted pyridine increases, the vertical EA decreases, ranging from 1.56 eV for **7** to 0.68 eV for **1**. Attempts to compute reduction potentials by adding solvation free energies to computed electron affinities failed to lead to a strong correlation with the experimental data, although this approach has proven effective in prior studies of chlorinated hydrocarbon reduction potentials.[49−55] The primary difficulty appears to be associated with the small variation of the experimental data (0.25 eV), which is on the order of the expected errors in solvation free energies for the anionic reduction products.[38] Another potential problem in making a comparison to experiment is that the reduction is irreversible, and it is not obvious that the theoretical model corresponds to the peak potential. In order to obtain more physical insights into the reductive bond cleavage, we decided to focus our theoretical efforts directly on the dissociative reaction coordinate.

(48) Van Den Bergen, A. M.; Elliott, R. L.; Lyons, C. J.; Mackinnon, K. P.; West, B. O. *J. Organomet. Chem.* **1985**, *297*, 361−370.
(49) Patterson, E. V.; Cramer, C. J.; Truhlar, D. G. *J. Am. Chem. Soc.* **2001**, *123*, 2025−2031.
(50) Nonnenberg, C.; van der Donk, W. A.; Zipse, H. *J. Phys. Chem. A* **2002**, *106*, 8708−8715.
(51) Bylaska, E. J. *Theor. Chem. Acc.* **2006**, *116*, 281−296.
(52) Arnold, W. A.; Winget, P.; Cramer, C. J. *Environ. Sci. Technol.* **2002**, *36*, 3536−3541.
(53) Lewis, A.; Bumpus, J. A.; Truhlar, D. G.; Cramer, C. J. *J. Chem. Educ.* **2004**, *81*, 596−604.
(54) Bylaska, E. J.; Dixon, D. A.; Felmy, A. R.; Apra, E.; Windus, T. L.; Zhan, C. G.; Tratnyek, P. G. *J. Phys. Chem. A* **2004**, *108*, 5883−5893.
(55) Winget, P.; Cramer, C. J.; Truhlar, D. G. *Theor. Chem. Acc.* **2004**, *112*, 217−227.

Table 3. Reaction Energies (kcal/mol) of Homolytic and Heterolytic Co−C Cleavage in Both the Gas Phase and with a Solvation Correction for DMSO

		Gas Phase		DMSO Solution	
	R group	homolytic	heterolytic	homolytic	heterolytic
4	*cis*-CCl=CHCl	57.6[a]	21.3	39.4	2.9
		55.0	18.5	36.8	0.1
		56.5	21.0	38.3	2.6
		45.4	25.7	27.2	7.2
8	$CH=CH_2$	41.4	43.5	30.4	9.2
		39.4	40.3	28.5	6.0
		41.1	42.8	30.2	8.5
		36.2	54.4	25.2	20.2
9	CH_3	30.1	47.8	19.4	1.1
		28.7	44.1	17.9	−2.6
		30.2	46.0	19.5	−0.8
		26.1	58.6	15.4	11.9

[a] Energies are reported from top to bottom as B3LYP/6-31+G(d), counterpoise-corrected B3LYP/6-31+G(d), B3LYP/6-311+G(2df,p), and BP86/6-31+G(d).

Calculated Co−C Scission Pathway. After being reduced, the Co−C bond of the cobaloxime complexes can cleave in two different ways (Scheme 1). What we will call heterolytic cleavage produces a vinyl anion and a neutral, open-shell Co(II) species as products, while homolytic cleavage produces a vinyl radical paired with an anionic Co(I) complex. In the gas phase, bond breaking is always endoergic, but analysis of the overall reaction energies indicates homolytic cleavage to be preferred for methyl and vinyl substituents, while heterolytic cleavage is preferred for the *cis*-dichlorovinyl substituent (Table 3). This trend is a simple reflection of EAs; the bare methyl and vinyl anions are much stronger reducing agents in the gas phase than the Co(II) species, while the situation is reversed once the vinyl group is substituted with two electronegative chlorine substituents. After accounting for solvation effects, all three bond scission processes are predicted to prefer the anionic charge to reside on the departing organic fragment. Since the solvation free energy of an ion varies inversely with its effective radius, solvation favors placing the charge on the small organic fragments. The net solvation free energies are such that the methyl and dichlorovinyl heterolyses are predicted to be weakly endoergic, and the dichlorovinyl heterolysis is predicted to be more so. Inclusion of entropy effects would, of course, stabilize separated products relative to reactants in free energy.

As a technical point, we note that Jensen and Ryde[56] have compared B3LYP to the BP86[31,57] density functional for the prediction of bond dissociation energies in cobalamins. They found a consistent difference of about 12 kcal mol^{-1} between the two levels, with BP86 predicting stronger bonds than B3LYP. They examined two cases particularly relevant to our present work, both of which involved R = Me, the same dmg ligands used here, and alternative *trans*-nitrogen ligands. Compared to experiment,[58] B3LYP was found to underestimate the energies of homolytic cleavage (in this case, leading to a Co(II) species, as the starting cobaloxime has not been reduced) by 8 to 9 kcal mol^{-1}, while BP86 overestimated the same energies by about 4 kcal mol^{-1}. We provide BP86-predicted energies in Table 3 and note that differences between the two functionals are similar to those found by Jensen and Ryde; in particular, larger differences appear for reactions which lead to doublet Co(II) than for those which lead to singlet Co(I) or Co(III). However, the range of the predicted B3LYP and BP86 energies, which likely bracket a best estimate, do not influence our qualitative observation that, in solution, heterolytic dissociation is favored in every instance. Similarly, the magnitude of effects associated with accounting for basis set superposition error, either by a counterpoise procedure or by increasing the basis set size to 6-311+G(2df,p), does not affect our qualitative conclusions.

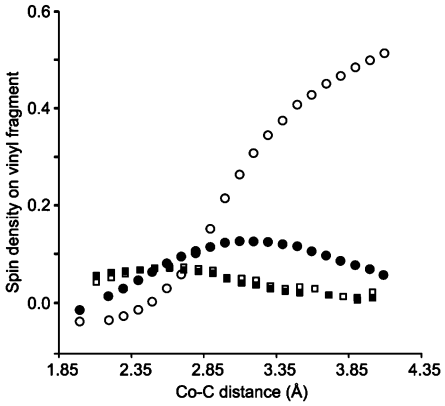

Figure 8. The spin densities (summed over all atoms) of the vinyl and *cis*-dichlorovinyl fragments along the Co−C dissociation reaction coordinate for one-electron reduced vinyl, **8**$^-$, and dichlorovinyl, **4**$^-$, complexes in both the gas phase (vinyl, open circles; *cis*-dichlorovinyl, open squares) and DMSO solution (vinyl, filled circles; *cis*-dichlorovinyl, filled squares).

Inspection of Mulliken partial atomic charges and spin densities along the Co−C bond dissociation reaction coordinates for all three substituents provides insight into the coupling between bond cleavage and charge transfer. As shown in Figure 8, as the Co−C bond is broken in **4**, there is almost no development of spin density on the dichlorovinyl fragment in either the gas phase or in solution, which indicates that the leaving group never exhibits radical character. Consistent with this interpretation is the rapid development of negative charge on the dichlorovinyl fragment in both the gas phase and solution as the bond is broken (Figure 9), with a fragment charge of nearly −1 being reached quite quickly in both cases.

The same analysis for the parent vinyl complex **8** contrasts with the dichlorovinyl case **4**. In the gas phase, as the Co−C distance increases, the spin density increases to ∼0.6 by the time 5 Å of separation is reached (Figure 8); given the energetic preference for homolytic dissociation in the gas phase, the curve must ultimately reach 1 at infinite separation. When solvation effects are included, the spin density does initially rise, but it begins to return to 0 beyond a separation of about 3 Å, again consistent with the preference for heterolytic dissociation in solution. Analysis of the vinyl fragment charge (Figure 9) leads to the same conclusions, that is, the vinyl group leaves as a radical in the gas phase and as an anion in solution.

(56) Jensen, K. P.; Ryde, U. *J. Phys. Chem. A* **2003**, *107*, 7539−7545.
(57) Perdew, J. P. *Phys. Rev. B* **1986**, *33*, 8822−8824.
(58) Halpern, J. *Science* **1985**, *227*, 869−875.

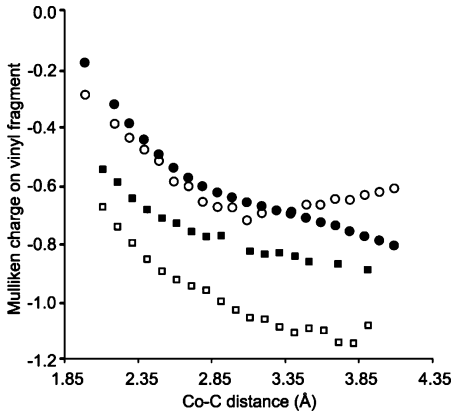

Figure 9. The Mulliken charge (summed over all atoms) of the vinyl and *cis*-dichlorovinyl fragments along the Co−C dissociation reaction coordinate for one-electron reduced vinyl, **8**$^-$, and dichlorovinyl, **4**$^-$, complexes in both the gas phase (vinyl, open circles; *cis*-dichlorovinyl, open squares) and DMSO solution (vinyl, filled circles; *cis*-dichlorovinyl, filled squares).

In the case of a methyl complex **9** (data not shown), the spin density of the methyl fragment rises quickly from 0 to a value near 1 in both the gas phase and in solution, and this situation persists out to 7 Å, beyond which point it becomes difficult to converge the SCF equations. Given the relative energetics of homolytic and heterolytic dissociation in solution (Table 3), this suggests that the reaction mechanism in the methyl case is homolytic dissociation followed by electron transfer.

We close by noting that prior theoretical studies on cobalamins have found that the relative energies of heterolytic Co−C bond dissociations are, in general, very sensitive to variations in *trans* ligands, while homolytic dissociations are largely insensitive.[59,60] Thus, replacement of the pyridine ligands studied here with other ligands might lead to different preferences for homo- versus heterolytic dissociation, although the predicted preference for dichlorovinyl is sufficiently large that this case seems likely to remain heterolytic under most conditions.

(59) Dölker, N.; Maseras, F.; Lledós, A. *J. Phys. Chem. B* **2001**, *105*, 7564−7571.
(60) Dölker, N.; Maseras, F.; Lledós, *J. Phys. Chem. B* **2003**, *107*, 306−315.

Conclusions

Based on DFT electronic structure calculations and an analysis of bond lengths across a series of complexes that vary in the electron demand of a bound pyridine ligand (L), we conclude that π-bonding is not important to metal−carbon bonds in *cis*-1,2-dichlorovinyl(L)cobaloxime complexes. Differences seen in the bond length and bond strength between alkyl and vinyl cobaloximes are, instead, due to the difference in hybridization of the cobalt-bound carbon. Theory was also used to determine whether reduction of *cis*-1,2-dichlorovinyl(pyridine)cobaloxime leads first to the *cis*-1,2-dichlorovinyl anion or the *cis*-1,2-dichlorovinyl radical. Analysis of the dissociation reaction coordinate indicates that the dichlorovinyl anion is formed directly from the reduced dichlorovinylcobaloxime complex and not via a radical intermediate. This work supports the view that radical intermediates, if formed in the cobalamin-mediated dechlorination of trichloroethylene, do not arise from reductive decomposition of a dichlorovinyl complex.

Acknowledgment. The authors thank Dr. Victor G. Young, Jr. of the University of Minnesota X-ray Crystallographic Facility for help with several of the crystal structures reported in this work. The authors also thank Sarah Kliegman and Glen Gullickson who solved the structures of compounds **2** and **7**, respectively, as part of CHEM 5755. This work was supported by the National Science Foundation (CHE-0239461 and CHE-0610183) and by the University of Minnesota through an Undergraduate Research Opportunities Program (UROP) grant to K.A.M.

Supporting Information Available: Structures of **1**−**7** optimized at the B3LYP/6-31+G(d) level. This material is available free of charge via the Internet at http://pubs.acs.org.

IC0618293